Seismic Retrofit Assessment of a School Building through Operational Modal Analysis and f.e. Modeling

Original
Seismic Retrofit Assessment of a School Building through Operational Modal Analysis and f.e. Modeling / Gara, F.; Carbonari, S.; Roia, D.; Balducci, A.; Dezi, L.. - In: JOURNAL OF STRUCTURAL ENGINEERING. - ISSN 0733-9445. - STAMPA. - 147:1(2021). [10.1061/(ASCE)ST.1943-541X.0002865]

Availability:
This version is available at: 11566/285066 since: 2024-11-28T09:01:34Z

Publisher:

Published
DOI:10.1061/(ASCE)ST.1943-541X.0002865

(Article begins on next page)

Seismic retrofit assessment of a school building through operational modal analysis and f.e. modelling

Fabrizio Gara[a], [1]Sandro Carbonari[a], Davide Roia[b], Alessandro Balducci[c], Luigino Dezi[a]

[a] Dept. ICEA, Università Politecnica delle Marche, Italy. E-mails: f.gara@univpm.it, s.carbonari@univpm.it, l.dezi@univpm.it

[b] Ph.D., Dept. ESD, University of San Marino, Republic of San Marino. E-mail: davide.roia@unirsm.sm

[c] SeiTec Seismotechnologies S.r.l., Italy. E-mail: balducci@seitec-srl.it

Abstract – The paper deals with the dynamic characterisation of a RC frame school building in central Italy before and after the seismic retrofitting, obtained by coupling the building with an innovative patented seismic dissipative protection system. Before the retrofit, ambient vibration tests were performed to evaluate frequencies and mode shapes for developing f.e. models describing the school dynamic behaviour in operational conditions. Several finite element models with increasing level of detail are presented, from the bare frame model, based on the assumptions and simplifications usually adopted for design purposes, to an upgraded model taking account of secondary and non-structural elements (e.g. internal and external walls, screeds, roofing, floor tiles and plasters) as well as the interaction between structure and retaining walls. The latter was used to develop the design model of the seismic retrofitting system, which aims to assure the immediate occupancy of the building in the case of severe earthquakes limiting damage to non-structural components. Tests were repeated after the retrofit to check consistency with numerical design predictions. Comparisons between experimental and numerical modal parameters are shown discussing the usefulness of ambient vibration tests.

Keywords: Building dynamic identification, ambient vibration test, operational modal analysis, RC frame building retrofitting, steel dissipative towers, finite element model upgrading

1. Introduction

Dynamic identification is an increasingly used technique in civil engineering, particularly for existing buildings. Generally, it is used: *i*) to calibrate structural models to be used for the design of

[1] Corresponding author. Dept. of Construction, Civil Engineering and Architecture, DICEA, Università Politecnica delle Marche, Via Brecce Bianche, 60131 Ancona, Italy - Tel.: + 39 071 2204547 E-mail address: s.carbonari@univpm.it

repair, rehabilitation and retrofit works; *ii*) to assess and validate structural design models for final testing; and *iii*) to monitor the structural health of buildings starting from the evaluation of changes in their dynamic behaviour over time. Various testing techniques differing in terms of equipment, time required, costs, and dynamic input can be adopted. However, Ambient Vibration Test (AVT) is one of the most attractive method for the evaluation of the dynamic characteristics of buildings due to its intrinsic advantages, such as the exploitation of ambient excitations as input instead of forced vibrations, the use of portable and light instrumentation and the possibility to carry out tests without disrupting buildings functionality. Due to the low amplitude range of vibrations ($\approx 10^{-5}$ g) produced by the ambient excitation, only the dynamic behaviour of the building at very small strains can be captured through AVTs.

Many ambient vibration tests have been executed in the last two decades for the dynamic identification of civil structures such as buildings, bridges, towers, (e.g. [1-10]) and many studies have been developed to assess factors affecting modal parameters (e.g. [11-12]). However, few examples can be found in literature regarding dynamic tests performed on civil structures before and after retrofitting works with the aim to validate a predictive f.e. structural model and to assess the dynamic behaviour variation due to the interventions (e.g. [13-19]). Indeed, data from AVTs (i.e. from tests that are able to capture the building dynamics only at small strains) are affected by contributions of non-structural components and can be profitably used to calibrate the linear behaviour of f.e. models in which nonlinearities can be later implemented to perform the seismic assessment of the retrofitted structures. Numerical models should be at least modified to account for the material nonlinearity and the contributions of non-structural components that during earthquake usually undergo damage that reduce interaction phenomena with the structural members.

Finally, although finite element model updating based on experimentally obtained modal parameters is a largely studied and well-known issue in civil engineering, only a few systematic researches concerning the effects of non-structural elements on the overall response of buildings are available in literature (e.g. [20-25]).

In this paper ambient vibration tests are exploited to assess a seismic retrofit of a strategic building. In details, the identification of the modal features of an existing low-rise RC frame school building before and after the seismic retrofit is presented discussing the f.e. model upgrading descending from the tests results. The upgraded model includes contributions of the in-plane deformability of floors, internal partitions, external infills and surrounding retaining walls. The specific contribution of the latter features on the overall dynamic structural behaviour is also shown and discussed. The refined model is adopted to design the retrofit system that is achieved with an innovative patented dissipative protection system called “Dissipative Towers” [26-28] that foresees the coupling of the existing building with new external rocking steel truss towers, pinned and equipped with viscous dampers at the base. The refined model, which accounts for both structural and non-structural components, was crucial for a proper design of the retrofitting system, which requires a reliable prediction of the building displacements subjected to severe earthquakes in order to limit damage to non-structural members. After the retrofit, the experimental dynamic response of the building is compared with the numerical predictions in terms of modal parameters (natural frequencies and mode shapes). Dynamic tests revealed important to (*i*) upgrade the design finite element model and (*ii*) to check that changes in the modal parameters due to the retrofit agreed with those predicted through the design model.

2 School building description

The school building is located in Camerino, in a high seismicity area in central Italy, as demonstrated by the recent Central Italy earthquake that struck the municipality in 2016. Figure 1 illustrates the plan view and sections of the RC building, which is composed of three blocks (Block A, Block B, and Block C) separated by expansion joints. Block A and Block C, constituted by a 4-storey 3 × 2 bay frame with an almost square plan (26.0 × 19.5 m), form the front of the building. Block B, at the rear of the building, has 3-storeys and a rectangular plan (12.85 × 28.20 m), and is constituted by frames with 2 bays of 4.0 m and 8.25 m in transverse direction and 7 bays of 3.6 m in longitudinal direction (Figure 2(a)); this part of the building was erected on ancient masonry walls constituting the lower part of a pre-existing structure.

The columns have 40 × 40 cm square cross sections rotated by 45° with respect to the frame plane. The beams on the building perimeter are linearly tapered with cross sections of about 30 × 80 cm and 30 × 40 cm at the beam-to-column joint and at mid-span, respectively, whereas the inner beams have constant rectangular cross sections with varying dimensions. The mean compressive strength of concrete is f_{cm} = 19.71 N/mm^2 and is obtained from an experimental investigation on 22 core samples extracted from structural elements. The joint between the blocks (red dashed lines in Figure 1(a)) regards only beams and columns (columns straddling the joint have a triangular cross section) while non-structural components (e.g. screeds, floors and infill walls) are continuous through the joints. RC floors are made of prefabricated beams and 20 cm high clay blocks, on which a 4 cm thick slab is cast. Infills of the external frames consist of 30 cm thick brick cavity walls with intermediate insulation having height of about 1.20 m from the floor (below windows), as shown in Figure 2(a). Internal partitions are mostly made with 8 cm thick hollow clay blocks, with plaster on both sides; occasionally, very light infill plasterboard partitions are also present.

2.1 The retrofit system and the need of dynamic tests for the design

Intrinsic geometry of beams and columns, as well as of infills, makes the building vulnerable to seismic actions, despite its social and strategic value. The seismic retrofit of the building was thus achieved through a patented dissipative protection system called “Dissipative Towers” [26-28]. In details, two external rocking steel truss towers pinned and equipped with viscous dampers at the base have been positioned in plan according to Figure 1(a). Towers interact with the building at the floor levels, except at the first one ((Figure 1(b) and Figure 2(a)), through steel members which are connected to steel plates anchored to the external frames. Steel members are erected on RC thick base plates that are centrally pinned through a spherical support to the foundations. Viscous dampers are arranged vertically between the base and foundation plates (one device per vertex for tower A and two for tower B), so that the rocking of the tower base, due to the building horizontal displacements, can activate all the devices. Dampers are included into an articulated quadrangle (Figure 2(b)) that amplifies the device displacements thanks to a leverage system. Furthermore, thick steel plates duly anchored to adjacent columns and beams are used to structurally connect adjacent blocks of the building.

From a conceptual point of view, the tower stiffness promotes a linear displacement profile and a constant inter-story drift, preventing soft-story collapses, while viscous dampers largely enhance the building dissipative capacity. Since the energy dissipation through dampers is very high, linear dynamic response spectrum analyses are not allowed to assess the seismic performance of the retrofitted system [29] and dynamic nonlinear analyses, involving the use of acceleration time histories, are required. However, nonlinearities are limited to dissipative devices since "Dissipative Towers" are dimensioned to assure a linear elastic behaviour of structural members. For the investigated case study, the retrofit system was designed not only to assure a linear behaviour of the building, but also to limit damage of non-structural elements in case of severe earthquakes (e.g. for actions normally corresponding to the life safety limit state) [29]. For this purpose, the design of the retrofitting system must be carried out suitably considering the overall initial stiffness of the building, which is largely affected by contributions of both structural and non-structural components. Indeed, the design numerical model should be able to accurately predict the building displacements and inter-storey drifts to which structural and non-structural damage are related.

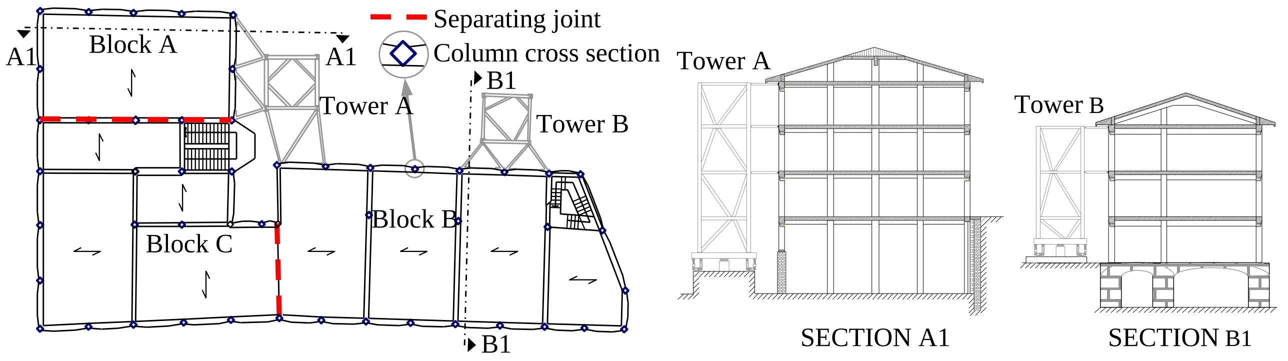

(a) (b)

Figure 1. (a) Plan view and (b) sections of the building.

(a) (b)

Figure 2. (a) Front and rear view of the school building; (b) viscous dampers at the base of the towers.

Thus, an estimation of the dynamic properties of the building in its operational condition (before the retrofit) is crucial for the development of a reliable numerical model that can be used for the retrofit design and, at the same time, a validation of the design model (i.e. including the retrofit system) is important, considering that the retrofit system must guarantee the building usability (with minor and fast repair interventions) after a severe earthquake.

3 Measurements and operational modal analysis

Ambient Vibration Tests (AVTs) are used to perform a dynamic characterization of the building before and after the retrofit. Modal information from tests executed before the retrofit were used to develop a numerical design model able to account for the building behaviour in its real service conditions while modal information from tests executed after the retrofit were used to validate the design model and its compliance with the real retrofitted structure.

3.1 Instrumentation and measurements

To measure the building vibrations due to ambient excitation, low noise piezoelectric accelerometers with a sensitivity of 10 V/g, a frequency range (± 10 %) of 0.07 ÷ 300 Hz, and a broadband resolution of 1 μg root mean square were used. Sensors were connected to a 24-bit data acquisition system with an input range of ± 5 V by means of low-noise coaxial cables. The maximum measurable accelerations were ± 0.5 g. A laptop with dedicated software was adopted to store and process the signals (Figure 3).

Three accelerometers per floor were used (Figure 4(a)) that are enough to draw the global mode shape of the building capturing the coupled roto-translational motions of floors assumed to be rigid in their plane. For each configuration, 1000-second long records, sampled at a rate of 2048 Hz (the lower limit allowed by the adopted acquisition system), were acquired. This time length largely exceeds the limit of about 1000-2000 times the fundamental period of the building, which is the acquisition length recommended to obtain an accurate estimate of the modal parameters with ambient vibration measurements [30]. In Figure 4(b) the time histories registered by accelerometers 2AX, 2AY and 2BX during one of the tests carried out before and after the retrofitting, are reported. The Root Mean Square (RMS) values of the measured accelerations are reported to show that the excitation levels during the measurements carried out before and after the retrofitting were comparable. RMS of the measured accelerations were calculated considering signal bands filtered in the frequency range that mainly characterise the dynamic behaviour of the building, i.e. 3-5 Hz.

For the measurements carried out before the retrofitting works, only 3 accelerometers were available, two of which, considered as references, were located at point A on the second floor (2AX and 2AY), while the third sensor (roving sensor) was moved around to all the other positions. For the analysis carried out after the retrofitting works, 12 accelerometers were available and only one configuration was necessary. However, three different acquisitions were carried out keeping the same sensor configuration, to better estimate the variability of the parameters identified thanks to data redundancy. Further details can be found by the reader in [31].

During tests, the air temperature and relative humidity were monitored outside the building; a temperature range of 19-22 °C and a relative humidity of about 60 % was observed during measurements carried out before the retrofitting works in August 2012 while a temperature range of 17-20 °C and a relative humidity of about 74 % was registered during tests performed after the retrofit in May 2013. Moreover, the wind velocity was quite low during both tests.

Figure 3. Measurement equipment during tests.

Figure 4. (a) Layout of accelerometers; (b) filtered acceleration time histories with RMS values, before and after retrofitting.

Environmental parameters, especially wind velocity and environmental temperature, are known to affect the modal parameters of structures [32-35]; however, considering similarities of excitation levels and environmental conditions relevant to the two tests, it can be concluded that changes in the modal parameters of the building can be almost completely attributed to effects of the retrofitting works.

3.2 Signal processing and operational modal analysis

Standard signal processing techniques were applied to all the recorded data before carrying out modal analyses. First, a correction of the spurious trends of signals was performed by subtracting the contribution resulting from the signals fitting with a third-degree polynomial. Then, the records were filtered with a low-pass filter with a cut-off frequency of 20 Hz to avoid aliasing phenomena. Finally, the signals were down-sampled at 51.2 Hz to reduce the number of data and make subsequent analyses faster. The modal parameters of the building (natural frequencies, damping ratios mode shapes) were identified using two output-only techniques implemented in Matlab environment [36]: the Enhanced Frequency Domain Decomposition (EFDD) method [37,38] and the Covariance-driven Stochastic Subspace Identification (SSI-COV) method [39-42]. Considering that very close results have been obtained with the two methods, only results from the SSI-COV method are herein presented. In this work, a model order of 50 is used and, in the stabilisation diagrams (Figure 5), a mode is assumed consistent with reference to frequency, damping ratio and mode shape when, by increasing the model order, it shows a natural frequency variation < 1% (green cross), a damping ratio variation < 2% (red circle), and a Modal Assurance Criterion (defined in the following section) MAC > 0.98 (cyan star), respectively.

Comparison between mode shapes

To compare mode shapes and obtained from measurements before and after the building retrofitting, the Modal Assurance Criterion (MAC) [43], was used.

Figure 5. Stabilisation diagrams (SSI-COV) for measurements before and after retrofitting works.

This criterion is defined as

(1)

and provides a numeric value that assesses the correspondence between two mode shapes. MAC value is 1 for perfectly matching mode shapes (parallel vectors) and 0 for completely different mode shapes (orthogonal vectors). In the following, MAC values are presented in matrix form exploiting a greyscale ranging from white (MAC = 0) to black (MAC = 1).

4 Modal features from ambient vibration tests

4.1 Tests before retrofitting

The left half side of Table 1 presents the resonance frequencies *f* and damping ratios ξ of the first seven modes identified before retrofitting. The values of damping ratios ξ relevant to the first seven modes vary between 0.9 and 2.6 %, showing a quite high variability, which is rather usual for buildings and civil engineering structures when identified through ambient vibration testing. As for mode shapes, a 3D isometric view is reported in Figure 6(a) (the last floor of block A is not included because it was not monitored). Furthermore, the basement results to be practically fixed since its modal displacements are negligible compared to those of the upper floors. The first three modes are those typical for low-rise RC frame buildings and can be assimilated to a first transverse mode with torsional component, a first torsional mode, and a first longitudinal mode with torsional component. A significant torsional component is always present due to the L-shaped plan of the building. The subsequent two mode shapes cannot be clearly assimilated to standard mode shapes while the sixth and the seventh are similar to the second torsional and transverse modes, respectively.

4.2 Tests after retrofitting

The right half side of Table 1 reports values of the natural frequencies f and the damping ratios ξ of the first seven modes identified while the identified mode shapes are shown in Figure 6(b). The latter appear like those obtained from tests executed before retrofitting and small differences cannot be clearly recognised through the graphical representation. The first three modes are again those typical of low-rise RC frame buildings: a first transverse mode, a first torsional mode, and a first longitudinal mode, all with a significant torsional component. The fifth and the sixth modes are assimilable to second modes, longitudinal and transverse, respectively.

4.3 Comparison between the results of the tests performed before and after retrofitting

Despite above mentioned similarities, significant changes in the building dynamic behaviour are found from the comparison of results obtained from tests performed before and after the seismic retrofit, denoted with subscripts *b* and *a*, respectively. It is worth noting that the modal parameters of real buildings identified by means of operational modal analysis at different times are generally affected by a certain variability.

Table 1. Modal parameters before and after retrofitting.

	Before		After		
mode	$f_{ex,b}$ [Hz]	$\xi_{ex,b}$ [%]	$f_{ex,a}$ [Hz]	$\xi_{ex,a}$ [%]	Mode shape
1st	3.61	1.46	3.60	1.49	first transverse
2nd	3.70	1.69	3.82	1.96	first torsional
3rd	4.00	1.14	4.14	1.49	first longitudinal
4th	4.41	0.92	5.00	1.17	/
5th	7.25	1.16	7.69	1.15	/
6th	8.69	2.58	9.54	2.18	/
7th	9.89	2.41	10.50	3.30	/

Figure 6. Resonance frequencies and mode shapes (a) before and (b) after retrofitting.

This is due not only to signal acquisition and processing but also to random changes in a number of factors such as amount and distribution of masses inside the building as well as environmental conditions (e.g. wind, temperature, humidity). However, these uncertainties generally induce much smaller variations in modal parameter values than those identified for the case under discussion.

Interesting considerations can arise when observing the changes in the values of resonance frequencies and damping ratios, as well as when comparing mode shapes [44]. To facilitate the reader, the values of the first seven resonance frequencies identified before and after the building retrofit are listed in Table 2. Except for the first mode, a general increase, ranging between 0.12 and 0.85 Hz, with an average value of about 6 % can be observed after the retrofit. This can be interpreted as a consequence of a general increase in the stiffness of the building coupled with steel towers. In particular, it is worth observing that the first resonance frequency is practically unchanged and that the second and the third frequencies undergo a small increment.

Table 2. Experimental resonance frequencies before ($f_{ex,b}$) and after ($f_{ex,a}$) the building retrofit.

mode	$f_{ex,b}$ [Hz]	$f_{ex,a}$ [Hz]	$(f_{ex,b}-f_{ex,a}) / f_{ex,b}$ [%]
1st	3.61	3.60	-0.2
2nd	3.70	3.82	3.0
3rd	4.00	4.14	3.6
4th	4.41	5.00	13.4
5th	7.25	7.69	6.1
6th	8.69	9.54	9.8
7th	9.89	10.45	5.7

Conversely, the higher frequencies present greater increments, particularly the fifth, the sixth and the seventh increase by about 6.1 %, 9.8 % and 5.7 %, respectively. This behaviour is consistent with the adopted retrofitting system that foresees stiff steel towers free to rotate at their base and only connected to the building in correspondence of the floors. As a consequence, towers do not add much stiffness with respect to modes that involve an almost-linear deflection of the building, i.e. the first three modes. Conversely, they strongly increase the stiffness with respect to higher modes that imply a non-linear deflection of the building vertical profile, i.e. with non-uniform values of inter-storey drift. Furthermore, the increase in the resonance frequency values is also partially due to the stitching of joints separating the building blocks (before the retrofit the interactions among blocks are only due to non-structural components). This effect is more pronounced for modes involving relative movements between blocks (e.g. the fourth), as will be shown later through a refined f.e. model of the structure.

Regarding damping ratios, typical values ranging between 1.5-3.0% are obtained, as usual for AVTs on RC low-rise buildings. It should be remarked that the dissipative contribution of the towers cannot be captured with AVTs, because dissipative devices are not activated by low amplitude vibrations. Finally, mode shapes identified before and after the building retrofit remain quite similar and the differences cannot be clearly identified graphically; thus, differences are captured analytically by means of MAC in Figure 7a. Very little differences can be observed for the first four modes while a variation in the higher modes (especially the fifth and the sixth) appears evident; this confirms considerations already made about changes of the natural frequencies, which are more evident for higher modes. Indeed, the rigid steel towers connected at the base through a spherical hinge contribute to linearize the profiles of horizontal displacements of the building. Thus, the tower-building interactions are more evident for higher modes, which are characterised by nonlinear profiles of horizontal displacements whereas effects on lower modes are less pronounced, since displacement profiles are closer to linearity. For lower modes, the contribution of the towers to the regularisation of mode shapes can be better appreciated by means of the MAC between the experimental mode shapes and a perfectly linear deflection.

Figure 7. (a) MAC between mode shapes before and after retrofitting; (b) profile of modal displacements at AX and AY before and after retrofitting, and MAC values with an ideal linear deflection of the building.

Figure 7b shows components of modal displacements of the first three modes in the two principal directions of the building in correspondence of alignments AX and AY for both the pre-retrofitted (blue lines) and retrofitted (red lines) conditions. In order to compare the profiles of modal displacements with respect to an ideal linear deflection of the building, MAC values between the experimental modal displacements and a linear trend are computed and reported in the figure with the relevant colour. A general increase in the MAC value, corresponding to a regularisation of the modes (i.e. mode shapes closer to a linear shape), is obtained, especially for the second and the third modes.

5 3D finite element models

5.1. Building before retrofitting

A predictive refined finite element model for the seismic retrofit design of the existing building was developed in SAP2000 code [45]. The numerical model is based on available structural drawings of the building and in-situ measurements as well as destructive and non-destructive tests on the structural materials, i.e. extraction of concrete core samples to estimate the strength and elastic modulus of concrete, sonic tests to control the homogeneity of concrete elements and surveys using an electromagnetic cover meter to investigate position, depth and size of steel reinforcement.

Beams and columns are modelled with 2-nodes frame elements while slabs and walls are schematised with 4-nodes shell elements having six degrees of freedom (dof) per node. Prismatic frame elements are used for columns and internal beam sections, whereas non-prismatic frame elements are chosen for tapered external beams. About the latter, the major moment of inertia (bending in vertical plane) of the cross section is assumed to vary along the beam axis with a parabolic law, whereas the minor moment of inertia (bending in horizontal plane) varies linearly. The shell elements are discretised into almost rectangular elements with an area of about 0.1 m^2. This value was obtained according to preliminary convergence analysis, by gradually reducing the shell size up to a non-significant variation in the values of the natural frequencies. To consider the stiffening effect due to the intersection of the members at the beam-to-column joints, rigid-end offsets equal to the 70% of the nominal overlapping length are assumed for frame elements connecting to the nodes. The columns of Block A and Block C are fully restrained at the building basement. Being the building founded on cemented sandstone, this assumption is assumed to be quite representative of the structural behaviour of the building at operational condition. The columns of Block B are, instead, rigidly connected to the shells of the masonry walls constituting the foundations.

The masses of the structural elements (i.e. RC beams and columns) are automatically computed by the software according to assigned frame element cross sections and material properties. The masses of the external walls are uniformly distributed along the perimeter beams, whereas the masses of the floors, composed of structural slabs and non-structural elements (screeds, roofing, floor tiles and plasters), as well as those of the internal partition walls and furniture (considered as equivalent distributed loads) are considered lumped at beams that are orthogonal to the slabs orientation. Live loads are not considered initially, in order to simulate the real condition of the building during the test and to allow the model validation through comparisons of numerical and experimental results; in

Table 3 the values of self-weight of both structural and non-structural elements are listed for completeness.

Materials are assumed to behave elastically, with properties reported in Table 4; the static Young's modulus of concrete is derived from the mean value of the concrete strength (f_{cm} = 19.71 N/mm^2) as suggested by the Italian Standards [29]. The reduced modulus of elasticity, $E_{c,red}$, is assumed to be 65% of the static modulus, while the dynamic modulus of elasticity is obtained by increasing the static modulus by about 20% [46], to capture the dynamic behaviour at very low amplitude vibrations. The values of the static elastic modulus and mass of the retaining walls, as well as those of internal and external walls, are chosen according to the Italian Standards [47], depending on the masonry typology. Due to the lack of information available in the literature, the dynamic modulus of elasticity is obtained by increasing the static modulus by 20%, analogously to the concrete.

The following six different models with increasing degree of accuracy are developed.

- **Mod. 0a** and **Mod. 0b** (Figure 8(a)) are the bare frame models usually developed for design purposes. The internal partitions and external walls are not modelled, a rigid diaphragm is considered for each floor (i.e. infinite in-plane stiffness and null out-of-plane stiffness of the slabs), stairs and foundation walls at the base of Block B are modelled with shells. For the verifications in terms of Ultimate Limit States (ULS), the reduced value of the static modulus of the elasticity of concrete, $E_{c,red}$, is considered to account for concrete cracking (Mod 0a), whereas, for the verifications in terms of Service Limit States, the full static value is usually adopted to consider uncracked concrete conditions. In this case, to detect the behaviour at very low strain levels during operational conditions (ambient vibrations), the dynamic elastic modulus $E_{c,dyn}$ is adopted (Mod 0b).

- **Mod. 1** takes account of the contribution of the external retaining wall by modelling the basements of Blocks A and C with shell elements, having dynamic modulus of elasticity $E_{rw,dyn}$, and by considering the stiffness contribution given by the soil surrounding the wall. The latter is included by means of supports restraining horizontal displacements and located at the first level in the front part of Blocks A and C.

Table 3. Loads of structural and non-structural members.

	Typical floor	Last floor	Roof	Stairs of block C	Stairs of block B
Structural [kN/m^2]	3.20	3.20	2.80	3.75	3.00
Non-structural [kN/m^2]	1.80	0.60	0.60	1.20	1.20
Non-structural [kN/m]	4.60				

Table 4. Elastic modulus [N/mm^2] and weight [kN/m^3] of concrete members and walls.

Concrete		Retaining wall		External wall		Internal wall	
$E_{c,st}$	25497	$E_{rw,st}$	3360	$E_{w,st}$	4583	$E_{w,st}$	3208
$E_{c,dyn}$	30720	$E_{rw,dyn}$	4032	$E_{w,dyn}$	5500	$E_{w,dyn}$	3850
$E_{c,red}$	16573	$E_{rw,red}$	/	$E_{w,red}$	/	$E_{w,red}$	/
w	25	w	22	w	20	w	12

- **Mod. 2** considers the in-plane deformability and bending stiffness of the floors by removing diaphragms and modelling slabs with anisotropic shells, which have inertia and stiffness characteristics equivalent to those of the reinforced concrete slab with a T-cross section coupled with screed and tiles, in the longitudinal direction, and to those of the slab flange coupled with screed and tiles, in the transverse direction. Furthermore, the self-weight plus other loads imposed on the floor are considered as uniform loads applied to the shells.

- **Mod. 3** takes into account the contributions of the internal partitions and external walls, which are modelled with shell elements having elastic modulus $E_{w,dyn}$ and thickness (masonry and plaster) of 0.12 m and 0.2 m, for internal partitions and external walls, respectively.

- **Mod. 4** (Figure 8(b)) accounts for the contribution of the soil surrounding the building; the supports located at the floor level are replaced with springs that are orthogonal to shells representative of the retaining walls. The spring stiffness is 8144 kN/m, corresponding to a subgrade reaction value of 80000 kN/m^3, according to Bowles [48], who suggests the range 80000-96000 kN/m^3 for a medium-dense sand. This final model is very accurate and rather complex, involving 2403 frame elements, 69291 shells, and 70743 nodes.

Numerical natural frequencies and mode shapes are obtained through an eigenvalue analysis and are compared with the experimental ones. Values of the natural frequencies of the first four modes of each model are graphically shown in Figure 9 proving a direct comparison with the corresponding experimental modes. For each model, the type of mode shape is also indicated, when it is clearly similar to a standard mode for buildings, i.e. transverse, longitudinal, and torsional modes, with reference to the directions *x* and *y* and to the rotation φ (around *z*), respectively.

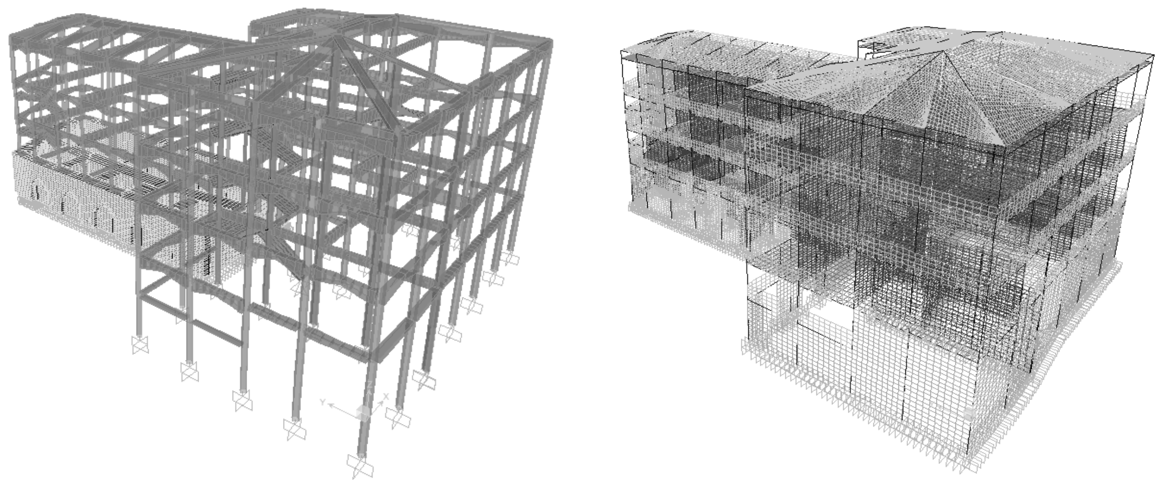

(a) (b)

Figure 8. 3D f. e. model of the building pre-retrofitting: (a) extruded view of the global model Mod.0a; (b) global model Mod. 4 (links not in view).

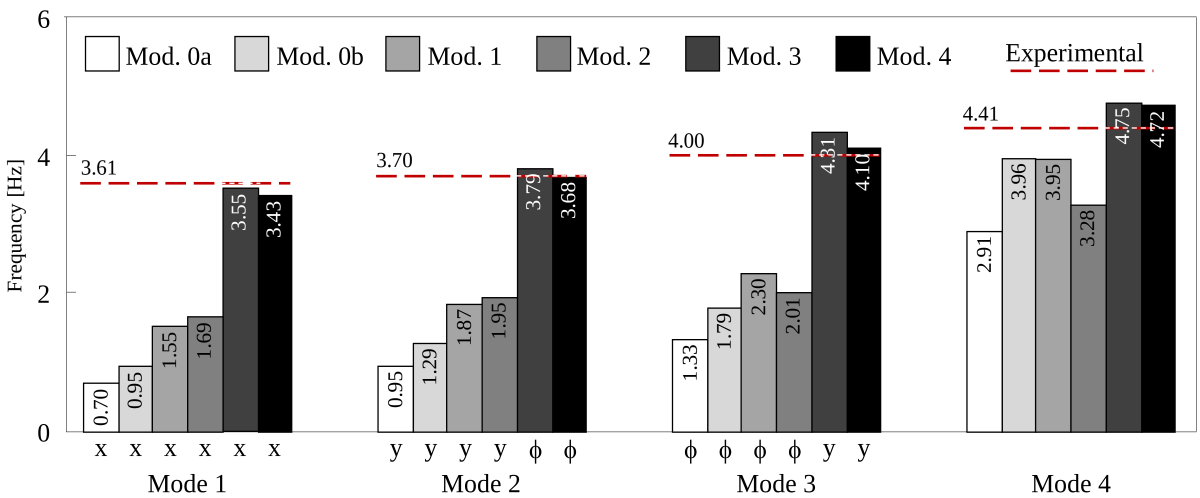

Figure 9. Natural frequencies obtained with f.e. models.

The bare frame model (Mod. 0a), usually adopted for structural design, shows values of natural frequencies much lower than the experimental ones (e.g. the first frequency is about one fifth). A significant increase in these theoretical values of about 30 % is obtained with Mod. 0b, thanks to a much higher value of the modulus of elasticity assumed for the concrete, $E_{c,dyn}$ instead of $E_{c,red}$ (increment of about 85%). It is worth noting that also the sequence of the modes disagrees with the experimental one: the first theoretical mode is mainly a transverse mode, the second is a longitudinal mode, and the third a torsional mode, whereas the first three experimental modes were mainly transverse, torsional and longitudinal modes, respectively. A further significant increase in the values of the first three natural frequencies (of about 63 %, 45 % and 28 %, respectively) is obtained with Mod. 1, thanks to the stiffening contribution given by the retaining walls and supports positioned at the ground level in the front part of the building.

With Mod. 2 a slight increase in the values of the first two natural frequencies is obtained, due to the bending stiffness of the shells introduced to model the floor. Vice versa, there is a decrease of about 13-17 % in the values of the third and the fourth natural frequencies that, being related to modes involving in-plane deformations of floors, are much more affected by the removal of the diaphragms that constrain the floor nodes avoiding in-plane deformations. It is worth noting that for all the models discussed so far, the longitudinal mode anticipates the torsional one in disagreement with the experimental results.

With Mod. 3 important modifications to the modal properties of the building are observed: the sequence of the modes now agrees with the experimental one, the values of the first three natural frequencies become almost twice those of Mod. 2 and quite close, even if slightly higher, to the experimental ones. These evidences confirm that the contribution of internal partitions and perimeter walls is of primary importance in the dynamic behaviour of the building for low-level vibrations.

Finally, Mod. 4, in which the supports located at the ground level are removed and the contribution of the soil surrounding the retaining wall is modelled with elastic springs, shows values of the natural frequencies that are slightly lower than those of Mod. 3 and close to the experimental ones.

Figure 10 shows the first seven mode shapes obtained with Mod. 4, whereas Table 5 illustrates the comparison between numerical (Mod. 4) and experimental modal parameters, i.e. the percentage difference between the values of natural frequencies and MAC values between mode shapes. A good agreement between numerical and experimental values of the natural frequencies is obtained, with a difference of about -5 % and -0.54 % for the values relevant to the first and the second modes and ranging between 2.50 % and 10.41 % for the higher modes.

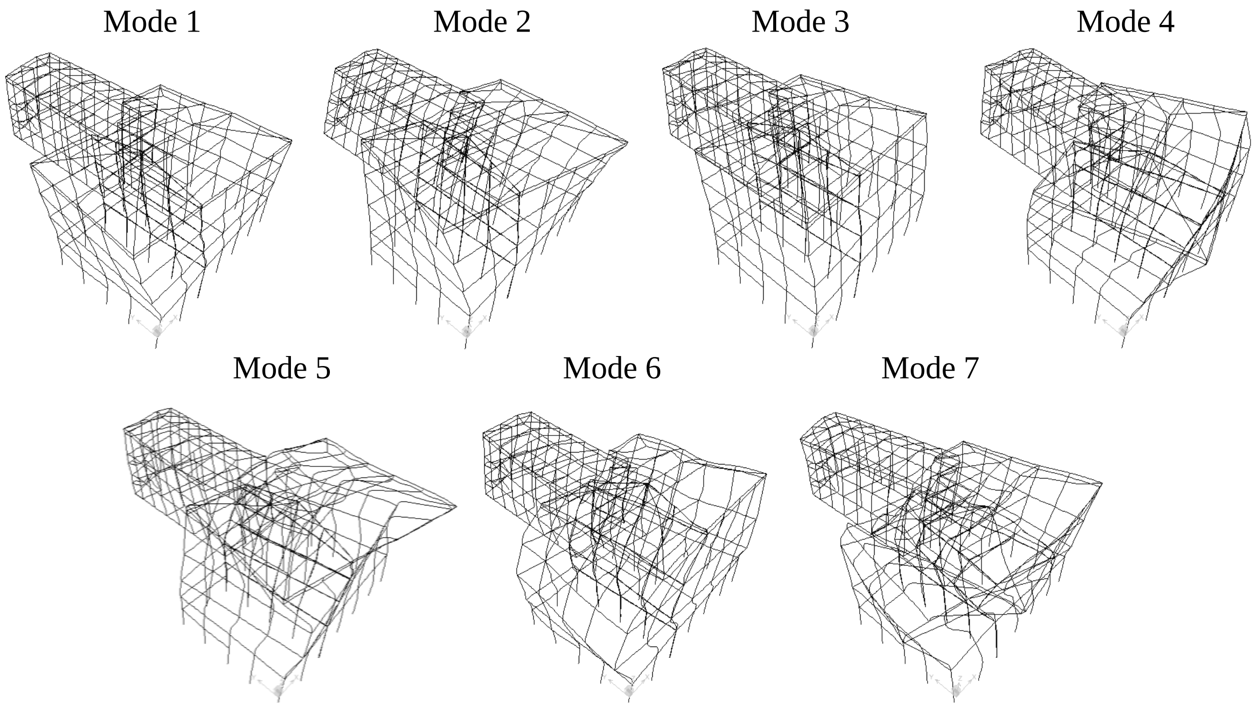

Figure 10. Mode shapes of Mod. 4 (shells and links not in view).

Table 5. Comparison between experimental and numerical (Mod. 4) modal parameters of the building before retrofitting.

	Experimental $f_{ex,b}$ [Hz]	Numerical $f_{n,b}$ [Hz]	$(f_n - f_{ex})_b$ / $f_{ex,b}$ [%]	MAC
1st mode	3.61	3.43	-4.99	0.93
2nd mode	3.70	3.68	-0.54	0.99
3rd mode	4.00	4.10	2.50	0.97
4th mode	4.41	4.72	7.03	0.98
5th mode	7.25	7.55	4.14	0.75
6th mode	8.69	9.07	4.37	0.72
7th mode	9.89	10.92	10.41	0.94

The MAC values show a very good correspondence with values ranging between 0.93 and 0.99 for the first four mode shapes and the seventh one, while higher modes present slightly lower values. It is worth mentioning that in practical applications the dynamic response of low-rise RC buildings is usually accurately estimated considering the contribution of the first modes.

5.2. Building after retrofitting

Starting from Mod. 4, a numerical finite element model that includes external towers and plates used to connect adjacent structural members close to the separating joints (Figure 11(a)) is developed and used for the retrofit design Hereafter, this model is referred to as Mod. 5 and is used for the estimation of the dynamic parameters of the retrofitted structure, which will be compared with results of experimental tests executed after the retrofit.

The steel towers are modelled with frame elements, while 0.5 m thick shell elements are used for the base plate. A hinge at the centroid of the intrados of the base plate restrains possible tower translations, while rotations are free. Articulated quadrangles that include dissipative devices, each modelled with two elastic frames (one horizontal and one vertical) and one link element, simulating the damper, are located at the vertexes of the base plate. The horizontal elastic frame is pinned at 1/3 of its length, while the vertical frame that includes the link is pinned both at the base plate and the horizontal frame (Figure 11(b)). Considering that the viscous dampers are not activated by very low amplitude vibrations as those registered during ambient vibration tests, the dissipative contribution of the devices is not accounted for. On the other hand, their elastic stiffening contribution is modelled by means of link elements. Assuming that the fluid inside the device does not flow between the two chambers of the device, the elastic stiffness K can be estimated, considering the fluid compressibility, as

(2)

where A (70.04 cm^2) and h (5.5 cm) are the cross section and the height of the fluid chamber, respectively, and B (105500 N/cm^2) is the bulk modulus of the viscous fluid. The towers are connected at each floor level, except for the first, by means of elastic elements hinged at the ends. Moreover, to model the intervention aimed at the structural connection of the three building blocks, frame elements are introduced to simulate the stiffness characteristics of the steel plates positioned on adjacent columns and beams, straddling the joints between two blocks. With regard to the materials, the values of the elastic moduli are assumed accordingly to the design parameters: E_a = 200000 MPa for the steel elements of the towers and $E_{c,d}$ =38770 MPa for the concrete of the base plates.

Table 6 presents a comparison between the modal parameters obtained from the numerical model and the experimental tests executed after the building retrofit in terms of percentage difference for frequencies and MAC values for the identified mode shapes (Figure 12). A good agreement between the numerical and experimental values of the natural frequencies is obtained, with a difference of less than 5% for values relevant to the first three modes as well as the fifth and the sixth. More scattered values are obtained for the fourth and the seventh modes. The MAC values show a very good correspondence for the first four mode shapes, with values ranging between 0.97 and 0.99, and a good agreement for the higher mode shapes, with values ranging between 0.80 and 0.86.

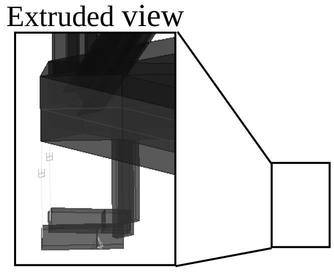

(a) (b)

Figure 11. 3D f. e. model of the building post-retrofitting: (a) global model Mod. 5 (links not in view); (b) detail of the dissipative system.

Table 6. Comparison between the experimental and numerical (Mod. 5) modal parameters of the building after retrofitting.

mode	Experimental $f_{ex,a}$ [Hz]	Numerical $f_{n,a}$ [Hz]	$(f_{n,a} / f_{ex,a})/ f_{ex,a}$ [%]	MAC
1st	3.60	3.48	-3.33	0.99
2nd	3.82	3.85	0.79	0.99
3rd	4.14	4.23	2.17	0.98
4th	5.00	5.57	11.40	0.97
5th	7.69	8.06	4.81	0.86
6th	9.54	9.41	-1.36	0.80
7th	10.45	11.87	13.59	0.86

Figure 12. Mode shapes of Mod. 5 (shells and links not in view).

5.3 Comparison between results of FE models before and after retrofitting

When comparing the numerical results obtained with Mod. 4 and Mod. 5 (building before and after retrofitting, respectively) in terms of natural frequencies (Table 7) and mode shapes by means of the MAC criterion, considerations analogous to those already made when discussing the experimental results hold. Due to the tower flexural stiffness and the structural connections of the building blocks, an increase in the natural frequencies of the building is observed.

Table 7. Comparison between the numerical modal parameters of the building before (Mod. 4) and after retrofitting (Mod. 5).

mode	$f_{n,b}$ [Hz]	$f_{n,a}$ [Hz]	$(f_{n,a},- f_{n,b}) / f_{n,b}$ [%]	MAC
1st	3.43	3.48	1.46	0.97
2nd	3.68	3.85	4.62	0.99
3rd	4.10	4.23	3.17	0.99
4th	4.72	5.57	18.01	1.00
5th	7.55	8.06	6.75	0.99
6th	9.07	9.41	3.75	0.99
7th	10.92	11.87	8.70	0.96

This increase is low for the first three modes ("linear" modes), ranging between 1.46 and 4.62 %, while it becomes more important for higher modes, with an increment ranging between 3.75 and 8.70 %. Finally, a significant increase of 18.01 % is observed for the fourth mode, as it involves in-plane relative rotations between the building blocks, which are more restrained after the retrofitting. With reference to mode shapes, values of MAC greater than 0.95 demonstrate that very small differences are observed for the first seven modes, consistently with the features of the protection system.

6 Conclusions

In this paper, the experimental and numerical modal properties of a school building before and after seismic retrofitting with external steel towers equipped with dissipative devices have been presented. Since the retrofitting system must guarantee the building usability after severe earthquakes, the design must be carried out with a model addressing the actual dynamic properties of the building, which strongly depends on both structural and non-structural members. In this framework, experimental modal parameters obtained from ambient vibration measurements are used to upgrade a conventional structural f.e. model of the building to be used for the retrofit design, including contributions of the in-plane deformability of floors, internal partitions, the external infills and the surrounding retaining walls. The role of the above usually neglected aspects on the overall dynamic structural behaviour is shown by progressively refining the building modelling.

Natural frequencies and mode shapes of the refined f.e. model are in good agreement with the experimental ones, with both reference to fundamental and higher modes, demonstrating the reliability of the model. The model was used for the design of the seismic protection system and provides the expected modal parameters of the retrofitted building that are used to assess the actual stiffening contributions of the retrofit.

By comparing the modal parameters of the building before and after retrofitting, an overall increase in the resonance frequencies has been observed. This increase is low for the first three modes (predominantly the first transverse, torsional and longitudinal modes), while it is more pronounced for the higher modes, as expected by numerical predictions. Furthermore, by comparing the mode shapes obtained before and after the building retrofit by means of the modal assurance criterion, it resulted that the first mode shapes remain almost unchanged while those related to the higher modes undergo greater variations, consistently with the peculiarities of the adopted protection system and the numerical expectations.

Overall, the dynamic identification of the building through ambient vibration tests revealed crucial for the development of a refined reliable f.e. model for the seismic protection system design, and the subsequent assessment of the actual stiffening contribution of the retrofit (dynamic proof test). This is of paramount importance when the seismic retrofit is designed to limit damage to non-structural components under seismic actions, because both structural and non-structural elements contribute to the overall dynamic response of the construction.

Data availability statement

Some or all data, models, or code that support the findings of this study are available from the corresponding author upon reasonable request.

References

[1] Ivanović S.S., Trifunac M.D., Novikova E.I., Gladkov A.A., Todorovska M.I. Ambient vibration tests of a seven-story reinforced concrete building in Van Nuys, California, damaged by the 1994 Northridge earthquake. Soil Dyn. Earthq. Eng., 19(6), 391–411, 2000.

[2] Liu K., Reynders E., De Roeck G., Lombaert G. Experimental and numerical analysis of a composite bridge for high-speed trains. Journal of sound and vibration, 320 (1-2), 201-220, 2009.

[3] Michel C., Guéguen P., El Arem S., Mazars J., Kotronis P. Full-scale dynamic response of an RC building under weak seismic motions using earthquake recordings, ambient vibrations and modelling. Earthq. Engng. Struct. Dyn., 39, 419-441, 2010.

[4] Oliveira C.S. and Navarro M. Fundamental periods of vibration of RC buildings in Portugal from in-situ experimental and numerical techniques. Bull. Earthquake Eng., 8, 609-642, 2010.

[5] Monitoring historical masonry structures with operational modal analysis: two case studies LF Ramos, L Marques, PB Lourenço, G De Roeck, A Campos-Costa, J Roque Mechanical systems and signal processing 24 (5), 1291-1305, 2010

[6] Zonta D., Wu H., Pozzi M., Zanon P., Ceriotti M., Mottola L., Picco G.P., Murphy A.L., Guna S., Corrà M. Wireless sensor networks for permanent health monitoring of historic buildings. Smart Structures and Systems, 6 (5-6), 595-618, 2010.

[7] Saisi A., Gentile C., Guidobaldi M. Post-earthquake continuous dynamic monitoring of the Gabbia Tower in Mantua, Italy. Construction and Building Materials, 81, 101-112, 2015.

[8] Ubertini F., Comanducci G., Cavalagli N. Vibration-based structural health monitoring of a historic bell-tower using output-only measurements and multivariate statistical analysis. Structural Health Monitoring, 15 (4), 439-457, 2016.

[9] Cabboi A., Gentile C., Saisi A. From continuous vibration monitoring to FEM-based damage assessment: Application on a stone-masonry tower. Construction and Building Materials, 156, 252-265, 2017.

[10] Gara F., Regni M., Roia D., Carbonari S., Dezi F. Evidence of coupled soil-structure interaction and site response in continuous viaducts from ambient vibration tests. Soil Dynamics and Earthquake Engineering, 120, 408-422, 2019.

[11] Moaveni B., Barbosa A. R., Conte J. P., Hemez F. M. Uncertainty analysis of system identification results obtained for a seven-story building slice tested on the UCSD-NEES shake table. Structural Control & Health Monitoring, 21 (4), 466-483, 2014.

[12] Behmanesh I., Yousefianmoghadam S., Nozari A., Moaveni B., Stavridis A. Uncertainty quantification and propagation in dynamic models using ambient vibration measurements, application to a 10-story building. Mechanical Systems and Signal Processing, 107, 502-514, 2018.

[13] Rodrigues J., Ledesma M. Modal identification of a viaduct before and after retrofitting works. Proc. of 25th Int. Modal Analysis Conf., Orlando FL, USA, 2007.

[14] Cunha A., Magalhães F., Caetano E. Output-only modal identification of Luiz I bridge before and after rehabilitation. Proc. Int. Conf. on Noise and Vibration Engng., Leuven, Belgium, September 2006.

[15] Antonacci E., Beolchini G.C., Di Fabio F., Gattulli V. Retrofitting effects on the dynamic behaviour of S.Maria di Collemaggio. Proc. of 10th Int. Conf. on Computational Methods and Experimental Measurements, Alicante, Spain, 2001.

[16] Takada T., Iwasaki R., An D.D., Itoi T., Nishikawa N. Dynamic behavior change of buildings before and after seismically retrofitting. 13th World Conf. on Earthquake Engineering, Vancouver, Canada, Paper No. 1237, 2004.

[17] Niousha A., Motosaka M. System identification and damage assessment of an existing building before and after retrofit. Journal of Structural Engineering (Japan), vol. 53B, 297-304, 2007.

[18] Ercan E. Assessing the impact of retrofitting on structural safety in historical buildings via ambient vibration tests. Construction and Building Materials, 164, 337-349, 2018.

[19] Soyoz S., Taciroglu E., Orakcal K., Nigbor R., Skolnik D., Lus H., Safak E. Ambient and forced vibration testing of a reinforced concrete building before and after its seismic retrofitting. Journal of Structural Engineering, 139(10), 1741-1752, 2013.

[20] Su R.K.L., Chandler A.M., Sheikh M.N., Lam N.T.K. Influence of non-structural components on lateral stiffness of tall buildings. Structural Design of Tall and Special Buildings, 14(2), 143–164, 2005.

[21] Pan T.C., You X., Brownjohn J.M.W. Effects of infill walls and floor diaphragms on the dynamic characteristics of a narrow-rectangle building. Earthquake Engineering and Structural Dynamics, 35(5), 637–651, 2006.

[22] Bakir P.G. Instrumentation and system identification of a typical school building in Istanbul. Structural Engineering and Mechanics 43(2), 2012.

[23] Butt F., Omenzetter P. Seismic response trends evaluation and finite element model calibration of an instrumented RC building considering soil–structure interaction and non-structural components. Engineering Structures, 65, 111-123, 2014.

[24] Astroza R., Ebrahimian H., Conte J.P., Restrepo J.I., Hutchinson T.C. Influence of the construction process and nonstructural components on the modal properties of a five-story building. Earthquake Engineering and Structural Dynamics, 45(7), 1063–84, 2016.

[25] O'Reilly G.J., Perrone D., Fox M., Lanese I., Monteiro R., Filiatrault A., Pavese A. (2019) System identification and seismic assessment modelling implications for Italian School Buildings. Journal of performance of constructed facilities, 33(1).

[26] Balducci A. Dissipative Towers. Application n. EP20100747238 20100831, WO2010EP62748 20100831, International and European classification E04H9/02 – Italian concession n° 0001395591, 2005.

[27] Gioiella L, Tubaldi E., Gara F., Dezi L., Dall'Asta A. Stochastic Seismic Analysis and Comparison of Alternative External Dissipative Systems. Shock and Vibration, 18, article ID 5403737, 2018.

[28] Gioiella L, Tubaldi E., Gara F., Dezi L., Dall'Asta A. Modal properties and seismic behaviour of buildings equipped with external dissipative pinned rocking braced frames. Engineering Structures, 172, 807-819, 2018.

[29] D.M.14.01.2018, Nuove Norme Tecniche per le Costruzioni, Ministero delle Infrastrutture, 17.01.2018 (in Italian).

[30] Cantieni R. Experimental methods used in system identification of civil engineering structures. Proc. 1st Int. Operational Modal Analysis Conf., Copenhagen, Denmark, pp. 249-260, 2005.

[31] Roia D., Gara F., Balducci A., Dezi L. Ambient vibration tests on a reinforced concrete school building before and after retrofitting works with external steel "dissipative towers". In Proc. of the 9th Int. Conf. on Structural Dynamics (EURODYN 2014), 30 June - 2 July 2014, Portugal.

[32] Ramos L.F., Marques L., Lourenço P.B., De Roeck G., Campos-Costa A., Roque J. Monitoring historical masonry structures with operational modal analysis: two case studies Mechanical systems and signal processing 24 (5), 1291-1305, 2010.

[33] Regni M., Arezzo D., Carbonari S., Gara F., Zonta D. Effects of Environmental Conditions on the Modal Response of a 10-Story Reinforced Concrete Tower. Shock and Vibration, 18, article ID 9476146, 2018.

[34] Xu D., Banerjee S., Wang Y., Huang S., Cheng X. Temperature and loading effects of embedded smart piezoelectric sensor for health monitoring of concrete structures. Construction and Building Materials, 76, 187-193, 2015.

[35] Ubertini F., Comanducci, G., Cavalagli, N., Pisello, L. A., Materazzi, L. A, Cotana, F. Environmental effects on natural frequencies of the San Pietro bell tower in Perugia, Italy, and their removal for structural performance assessment. Mechanical Systems and Signal Processing, 82, 307-322, 2017.

[36] MathWorks, MATLAB, version 7.9 (R2009b), The MathWorks Inc., Natick, Massachusetts. 2009.

[37] Brincker R., Ventura C.E., Andersen P. Damping estimation by frequency domain decomposition. Proc. of 19th Int. Modal Analysis Conf., Kissimmee, FL, USA, 698-703, 2001.

[38] Jacobsen N.J., Andersen P., Brincker R. Eliminating the influence of harmonic components in operational modal analysis. Proc. of 24th Int. Modal Analysis Conference, Orlando, FL, USA, 2007.

[39] Juang J.-N. Applied System Identification. Prentice-Hall Englewood Cliffs, New Jersey, USA, 1994.

[40] Van Overschee P., De Moor B. Subspace identification for linear systems: theory–implementation–applications. Dordrecht, The Netherlands: Kluwer Academic Publishers, 1996.

[41] Peeters B., De Roeck G. Reference-based stochastic subspace identification for output-only modal analysis. Mech Syst Signal Process 13(6):855–878, 1999.

[42] Peeters B. System Identification and Damage Detection in Civil Engineering. PhD Thesis, K. U. Leuven, Belgium, 2000.

[43] Allemang R.J., Brown D.L. A correlation coefficient for modal vector analysis. Proc. of 1st Int. Modal Analysis Conf., Bethel, CT, USA, 110–15, 1982.

[44] Zonta D., Elgamal A., Fraser M., Nigel Priestley M.J. Analysis of change in dynamic properties of a frame-resistant test building. Engineering Structures, 30 (1), 183-196, 2008.

[45] SAP2000 advanced (v15.0.0) Static and dynamic finite element analysis of structures, Berkeley, CSI Computer & Structures, Inc., 2009.

[46] Lydon F.D., Balendran R.V. Some Observations on Elastic Properties of Plain Concrete. Cement and Concrete Research, 16(3), 314-324, 1986.

[47] Repubblica Italiana, Consiglio Superiore dei Lavori Pubblici, Istruzioni per l'applicazione delle Nuove norme tecniche per le costruzioni di cui al decreto ministeriale 17 gennaio 2018. Circolare 21 gennaio 2019, n. 7. (in Italian)

[48] Bowles J.E. Foundation analysis and design, New York: McGraw-Hill, 1996.